

Optical properties of a Brane-World black hole as photons couple to the Weyl tensor

He-Xu Zhang, Cong Li, Peng-Zhang He, Qi-Qi Fan, and Jian-Bo Deng*

Institute of Theoretical Physics & Research Center of Gravitation,

Lanzhou University, Lanzhou 730000, China

(Dated: March 10, 2020)

Abstract

In this article, we have investigated the equations of motion of the photons coupled to Weyl tensor by the geometric optics approximation and the corresponding shadow in a Brane-World black hole spacetime. It is shown that there exists a double shadow for a black hole since the coupling photons with different polarization directions propagate along different paths in the spacetime. Furthermore, we discuss the effects of the metric parameter α related to the cosmological constant, X-cold dark matter parameter β and the coupling parameter λ on the umbra (the overlap region of the double shadow) and the penumbra. We also obtain the finite-distance corrections to the deflection angle of light in the Brane-World black hole spacetime as the photons coupled to Weyl tensor by using a recent geometric method.

PACS numbers: 04.70.Dy, 95.30.Sf, 97.60.Lf

* Jian-Bo Deng: dengjb@lzu.edu.cn

I. INTRODUCTION

In the context of the unification of the physical forces and also in cosmology, the extra dimensions models have been increasing interest during recent years. Among them the Brane-World cosmological models [1–3], motivated by string theory (M-theory), have been proposed in which the standard fields are confined to a four-dimensional (4D) world viewed as a hypersurface (the brane) embedded in a higher-dimensional space-time (the bulk) through which only gravity can propagate [4, 5]. With the help of the brane scenario, one could possibly solve some disturbing problem of high-energy physics, such as the hierarchy problems (the problem of the big difference between the electroweak scale $M_{EW} \sim 1$ TeV and the Planck scale $M_{pl} \sim 10^{16}$ TeV) and the cosmological constant problem [6–11]. As the most well-known model in the Brane-World theory, Randall and Sundrum (RS) models [8, 9] achieve the confine of the standard fields through the imposition of Z_2 symmetry and use of the Israel junction conditions which relates the extrinsic curvature of the brane to the energy-momentum tensor of the matter. However, this method works only when the theories have one extra dimension. In Ref. [12], Heydari-Fard and Razmi studied a Brane-World embedded in a m -dimensional bulk by means of the confining potential. The field equations obtained on the brane contained an extra term which was identified with the X-cold dark matter. The same method was used in [13, 14] to find the spherically symmetric vacuum solutions of the field equations on the brane. These solutions could account for the accelerated expansion of the universe and offered an explanation for the galaxy rotation curves without assuming the existence of dark matter and without working with modified Newtonian dynamics.

The interactions between electromagnetic field and curvature tensor are not included in the standard Einstein-Maxwell theory. Drummond et al. [15] first found that such kind of the couplings could be appeared naturally in quantum electro-

dynamics with the photon effective action originating from one-loop vacuum polarization on a curved background spacetime. The coupling between electromagnetic field and curvature tensor change the propagation path and dispersion relation of the coupled photons in spacetime which lead to the birefringence of light in the gravitational field and may result in the superluminal phenomenon in some cases [16, 17]. It is also found that the quantum fluctuation of electromagnetic field caused by the coupling of electromagnetic field and spacetime curvature can cause inflation in the early evolution of the universe [18–22]; the fluctuation of the electromagnetic field coupled with the gravitational field can also provide a possible physical mechanism for generating large-scale magnetic fields in the center of the Milky Way [23–26].

Since Weyl tensor is actually related to the curvature tensors $R_{\mu\nu\rho\sigma}$, the Ricci tensor $R_{\mu\nu}$ and the Ricci scalar R , the theory of electromagnetic field with Weyl corrections can be treated as a special kind of generalized Einstein-Maxwell theory with the coupling between the gravitational and electromagnetic fields. It is shown that the couplings with Weyl tensor change the universal relation with the $U(1)$ central charge in the holographic conductivity in the background of anti-de Sitter spacetime [27] and modify the properties of the holographic superconductor including the critical temperature and the order of the phase transition [28–34]. Moreover, Songbai Chen et al. find that with these couplings the dynamical evolution and Hawking radiation of electromagnetic field in the black hole spacetime depend on the coupling parameter and the parity of the field [35–37].

Due to the strong gravity and high mass density, the coupling between electromagnetic field and curvature tensor should be emerged reasonably in the region near the classical supermassive compact objects at the center of galaxies. Ni's model has been investigated widely in astrophysics [38–41] and black hole physics [42–44]. These investigations show that the coupling term modifies the equations of motion both for electromagnetic and for gravitational fields, which could yield time delays

in the arrival of gravitational and electromagnetic waves.

Recently, Songbai Chen studied the strong gravitational lensing for the photons coupled to Weyl tensor in Schwarzschild and Keer black hole spacetimes [45, 46]. And Yang Huang discussed the double shadow of a regular phantom black hole as photons couple to the Weyl tensor [47]. Abbas studied the strong gravitational lensing for photons coupled to Weyl tensor in Kiselev black hole [48]. In this work, we consider a Brane-World black hole spacetime described by Heydari-Fard and Razmi for which the shadow has not yet been calculated. We obtain the effective metric of the coupled photons by the geometric optics approximation, and then discuss the black hole shadow. We also calculate the deflection angle of light with finite-distance corrections in the Brane-World black hole spacetime as the photons coupled to Weyl tensor.

The plan of the paper is as follows. In the next section is the derivation of the equations of motion for the photons coupled to the Weyl tensor in the Brane-World black hole. In Sec. III, we discuss the Weyl corrections to photon sphere radius and angular radius of the shadow. Sec. IV is the deflection angle of light with finite-distance corrections in the Brane-World black hole. Conclusions and discussions are presented in Sec. V.

II. EQUATIONS OF MOTION FOR THE PHOTONS COUPLED TO THE WEYL TENSOR IN THE BRANE-WORLD BLACK HOLE

In this paper, we begin with the action of the electromagnetic field coupled to Weyl tensor in the curved spacetime, which can be expressed as [27]

$$S = \int d^4x \sqrt{-g} \left[\frac{R}{16\pi G} - \frac{1}{4} (F_{\mu\nu} F^{\mu\nu} - 4\lambda C^{\mu\nu\rho\sigma} F_{\mu\nu} F_{\rho\sigma}) \right], \quad (1)$$

where the electromagnetic tensor $F_{\mu\nu}$ is equal to $F_{\mu\nu} = A_{\mu;\nu} - A_{\nu;\mu}$ and λ is the coupling constant with dimension of length-squared. Note that $C_{\mu\nu\rho\sigma}$ is the Weyl tensor, which is defined as

$$C_{\mu\nu\rho\sigma} = R_{\mu\nu\rho\sigma} - (g_{\mu[\rho}R_{\sigma]\nu} - g_{\nu[\rho}R_{\sigma]\mu}) + \frac{1}{3}Rg_{\mu[\rho}g_{\sigma]\nu}, \quad (2)$$

here the brackets around indices refer to the antisymmetric part. Varying the action Eq. (1) with respect to A_μ , one can obtain the following Maxwell equations with Weyl correction

$$\nabla_\mu (F_{\mu\nu} - 4\lambda C_{\mu\nu\rho\sigma} F^{\rho\sigma}) = 0. \quad (3)$$

In order to derive the equations of motion of the photons from the above corrected Maxwell equations, one can adopt to the geometric optics approximation. Under this approximation, the wavelength of photon λ is much smaller than a typical curvature scale L , but is larger than the electron Compton wavelength λ_e , which ensures that the change of the background gravitational and electromagnetic fields with the typical curvature scale can be neglected for the photon propagation [15–17, 49–54]. In the geometric optics approximation, we write the electromagnetic field strength as the product of a slowly varying amplitude and a rapidly varying phase, i.e.

$$F_{\mu\nu} = f_{\mu\nu} e^{i\theta}, \quad (4)$$

where the wave vector is $k_\mu = \nabla_\mu \theta$. In the quantum particle interpretation, we identify it as the photon momentum. The amplitude is constrained by the Bianchi identity to be of the form

$$f_{\mu\nu} = k_\mu a_\nu - k_\nu a_\mu, \quad (5)$$

where a_μ is the polarization vector satisfying the condition that $k_\mu a^\mu = 0$. Light rays (photon trajectories) are defined as the integral curves of the wave vector (photon

momentum). Substituting Eqs. (4) and (5) into Eq. (3) and using the relationship above, we can get the equation of motion of photon coupling to the Weyl tensor

$$k_\mu k^\mu a^\nu + 8\lambda C^{\mu\nu\rho\sigma} k_\sigma k_\mu a_\rho = 0. \quad (6)$$

Obviously, the coupling term with Weyl tensor changes the propagation of the coupled photon in the background spacetime. It is convenient to introduce the orthonormal frame by using the vierbeins defined as $g_{\mu\nu} = \eta_{ab} e_\mu^a e_\nu^b$, where η_{ab} is the Minkowski metric. In the orthonormal frames, Eq. (6) can be rewritten as

$$k^2 a^b + 8\lambda C^{abcd} k_d k_a a_c = 0. \quad (7)$$

As mentioned above, Heydari-Fard and Razmi have gotten a black hole solution with X-cold dark matter in Brane-World theory described by the spacetime metric [12]

$$ds^2 = -f(r) dt^2 + \frac{dr^2}{f(r)} + r^2 (d\theta^2 + \sin^2\theta d\phi^2), \quad (8)$$

with

$$f(r) = 1 - \frac{2M}{r} - \alpha^2 r^2 - 2\alpha\beta r - \beta^2. \quad (9)$$

Here, α is a metric parameter which is related to the cosmological constant and β is a parameter of X-cold dark matter. It is the Schwarzschild-de Sitter-like solution as $\beta = 0$ and the Schwarzschild- Λ CDM solution as $\alpha = 0$.

We now introduce a local orthonormal frame. The appropriate basis 1-forms are e^a ($a = 0, 1, 2, 3$) with

$$e^0 = \sqrt{f} dt, \quad e^1 = \frac{1}{\sqrt{f}} dr, \quad e^2 = r d\theta, \quad e^3 = r \sin\theta d\phi. \quad (10)$$

By a straightforward calculation, in the orthonormal frame the independent nonvanishing components of the Riemann curvature tensor are

$$\begin{aligned} R_{0101} &= -\frac{2M}{r^3} - \alpha^2, & R_{0202} &= R_{0303} = \frac{M}{r^3} - \frac{\alpha\beta}{r} - \alpha^2, \\ R_{1212} &= R_{1313} = -\frac{M}{r^3} + \frac{\alpha\beta}{r} + \alpha^2, & R_{2323} &= \frac{2M}{r^3} + \frac{\beta^2}{r^2} + \frac{2\alpha\beta}{r} + \alpha^2. \end{aligned} \quad (11)$$

Introducing the notation $U_{ab}^{01} \equiv \delta_a^0 \delta_b^1 - \delta_a^1 \delta_b^0$, etc., one can rewrite the complete Weyl tensor compactly in the following form

$$C_{abcd} = \mathcal{A} (2U_{ab}^{01}U_{cd}^{01} - U_{ab}^{02}U_{cd}^{02} - U_{ab}^{03}U_{cd}^{03} + U_{ab}^{12}U_{cd}^{12} + U_{ab}^{13}U_{cd}^{13} - 2U_{ab}^{23}U_{cd}^{23}), \quad (12)$$

with

$$\mathcal{A} = - \left(\frac{M}{r^3} + \frac{\beta^2}{6r^2} \right). \quad (13)$$

In order to solve the equation of motion for the coupled photon propagation, one can introduce three linear combinations of momentum components [17, 50]

$$l_b = k^a U_{ab}^{01}, \quad m_b = k^a U_{ab}^{02}, \quad n_b = k^a U_{ab}^{03}, \quad (14)$$

and some dependent combinations

$$p_b = k^a U_{ab}^{12}, \quad q_b = k^a U_{ab}^{13}, \quad r_b = k^a U_{ab}^{23}. \quad (15)$$

Using l_b , m_b , and n_b to contract Eq. (7), with the help of Eq. (12), the photon equations of motion coupling with Weyl tensor can easily be simplified as a set of equations for three independent polarisation components $a \cdot l$, $a \cdot m$ and $a \cdot r$

$$\begin{pmatrix} K_{11} & 0 & 0 \\ K_{21} & K_{22} & K_{23} \\ 0 & 0 & K_{33} \end{pmatrix} \begin{pmatrix} a \cdot l \\ a \cdot m \\ a \cdot r \end{pmatrix} = 0, \quad (16)$$

with

$$\begin{aligned} K_{11} &= (1 - 16\lambda\mathcal{A}) (-k^0 k^0 + k^1 k^1) + (1 + 8\lambda\mathcal{A}) (k^2 k^2 + k^3 k^3), \\ K_{21} &= -24\lambda\mathcal{A} k^1 k^2, \\ K_{22} &= (1 + 8\lambda\mathcal{A}) (-k^0 k^0 + k^1 k^1 + k^2 k^2 + k^3 k^3), \\ K_{23} &= 24\lambda\mathcal{A} k^0 k^3, \\ K_{33} &= (1 + 8\lambda\mathcal{A}) (-k^0 k^0 + k^1 k^1) + (1 - 16\lambda\mathcal{A}) (k^2 k^2 + k^3 k^3). \end{aligned} \quad (17)$$

The condition of Eq. (16) with non-zero solution is $K_{11}K_{22}K_{33} = 0$. The first root $K_{11} = 0$ leads to the modified light cone

$$(1 - 16\lambda\mathcal{A})(-k^0k^0 + k^1k^1) + (1 + 8\lambda\mathcal{A})(k^2k^2 + k^3k^3) = 0, \quad (18)$$

which corresponds to the case the polarisation vector a_μ is proportional to l_ν and the strength $f_{\mu\nu} \propto (k_\mu l_\nu - k_\nu l_\mu)$. The second root $K_{22} = 0$ means that $a \cdot l = 0$ and $a \cdot r = 0$ in Eq. (16), which implies $a_\mu = \lambda k_\mu$ and then $f_{\mu\nu}$ vanishes [15]. Thus, this root corresponds to an unphysical polarisation and it should be neglected for general directions of propagation of the coupled photon. The third root is $K_{33} = 0$, i.e.,

$$(1 + 8\lambda\mathcal{A})(-k^0k^0 + k^1k^1) + (1 - 16\lambda\mathcal{A})(k^2k^2 + k^3k^3) = 0, \quad (19)$$

which means that the vector $a_\mu = \lambda r_\mu$ and the strength $f_{\mu\nu} \propto (k_\mu r_\nu - k_\nu r_\mu)$.

It is easy to find that the light cone conditions Eq. (18) and Eq. (19) indicate that the motion of the coupled photons in the equatorial plane is non-geodesic in the Kerr metric. In fact, these photons follow null geodesics of the effective metric $\gamma_{\mu\nu}$, i.e., $\gamma^{\mu\nu}k_\mu k_\nu = 0$ [39]. Moreover, the effects of Weyl tensor on the photon propagation are different for the coupled photons with different polarizations, which yields a phenomenon of birefringence in the spacetime [16, 17, 49–51, 55].

The effective metric for the coupled photon in the standard Boyer-Lindquist coordinates can be expressed as

$$ds^2 = -f(r) dt^2 + \frac{dr^2}{f(r)} + W(r)^{-1} r^2 (d\theta^2 + \sin^2\theta d\phi^2). \quad (20)$$

The quantity $W(r)$ is

$$W(r) = \frac{6r^3 - 8\lambda(6M + \beta^2r)}{6r^3 + 16\lambda(6M + \beta^2r)}, \quad (21)$$

for photon with the polarization along l_μ (PPL) and

$$W(r) = \frac{6r^3 + 16\lambda(6M + \beta^2r)}{6r^3 - 8\lambda(6M + \beta^2r)}, \quad (22)$$

for photon with the polarization along r_μ (PPR), respectively.

III. WEYL CORRECTIONS TO PHOTON SPHERE RADIUS AND ANGULAR RADIUS OF THE SHADOW

A. Photon sphere radius

In this subsection, we will discuss the Weyl correction to photon sphere radius and angular radius of the shadow. For simplicity, we here just consider that the whole trajectory of the photon is limited on the equatorial plane $\theta = \frac{\pi}{2}$. Since the existence of cyclic coordinates t and ϕ in spacetime Eq. (20), we can obtain two constants of motion

$$E = f(r)\dot{t}, \quad L = r^2W(r)^{-1}\dot{\phi}, \quad (23)$$

where a dot represents a derivative with respect to affine parameter λ along the geodesics. E and L are, respectively, the energy and angular momentum of the photon.

Using the the null geodesics of the effective metric condition $\gamma^{\mu\nu}k_\mu k_\nu = 0$, one can find that

$$\left(\frac{dr}{d\lambda}\right)^2 = f(r) \left[\frac{E^2}{f(r)} - W(r) \frac{L^2}{r^2} \right]. \quad (24)$$

Combining Eq. (24) with $\frac{dr}{d\lambda} = 0$ and $\frac{d^2r}{d\lambda^2} = 0$, we obtain the photon sphere radius r_{ph} in the equatorial plane satisfying the condition

$$W(r)[rf'(r) - 2f(r)] + rW'(r)f(r) = 0. \quad (25)$$

First, as an example, we show the effect of parameter α related to the cosmological constant on the photon sphere radius r_{ph} and the angle radius θ_{sh} of the black hole shadow (the approach is given in the next subsection) for PPL in Table I. According to Table I, it is easy to find that the difference of θ_{sh} between $\alpha = 10^{-12}$ and $\alpha = 10^{-20}$ is of order $10^{-3} \sim 10^{-2} \mu as$, which far exceeds the angular resolution of

the Event Horizon Telescope (EHT) and the space-based very-long baseline interferometry (VLBI) RadioAstron [56, 57]. Therefore we only present the variation of r_{ph} with the coupling factor α and X-cold dark matter parameter β for PPL and PPR in Figs. 1 and 2, respectively.

α	10^{-12}	10^{-14}	10^{-16}	10^{-18}	10^{-20}
r_{ph}	1.639032	1.639032	1.639032	1.639032	1.639032
$\theta_{sh}(\mu as)$	29.2310	29.2931	29.2937	29.2937	29.2937

Table I. Dependence of r_{ph} and the angular radius of the shadow θ_{sh} on the parameter α related to the cosmological constant for PPL. Here we choose Sgr A* as an example and set $2M = 1$, $\beta = 0.1$, and $\lambda = 0.05$.

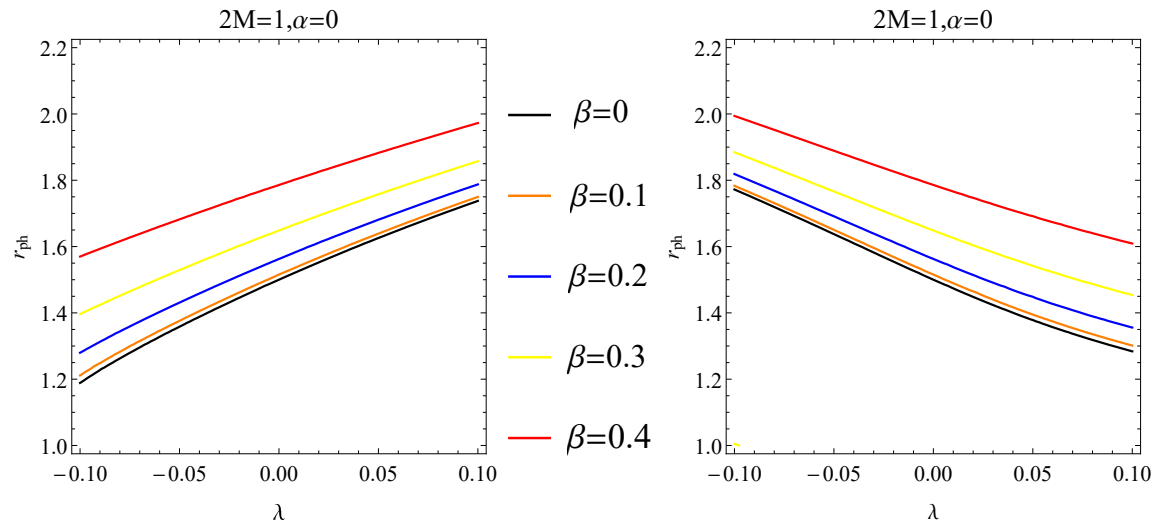


Figure 1. Variety of the photon sphere radius r_{ph} with the coupling constant λ in a Brane-World black hole spacetime. The left and the right are for PPL and PPR, respectively.

It is shown that, for different values of β , the photon sphere radius r_{ph} increases with the coupling parameter λ for PPL and decreases for PPR. Moreover, with the

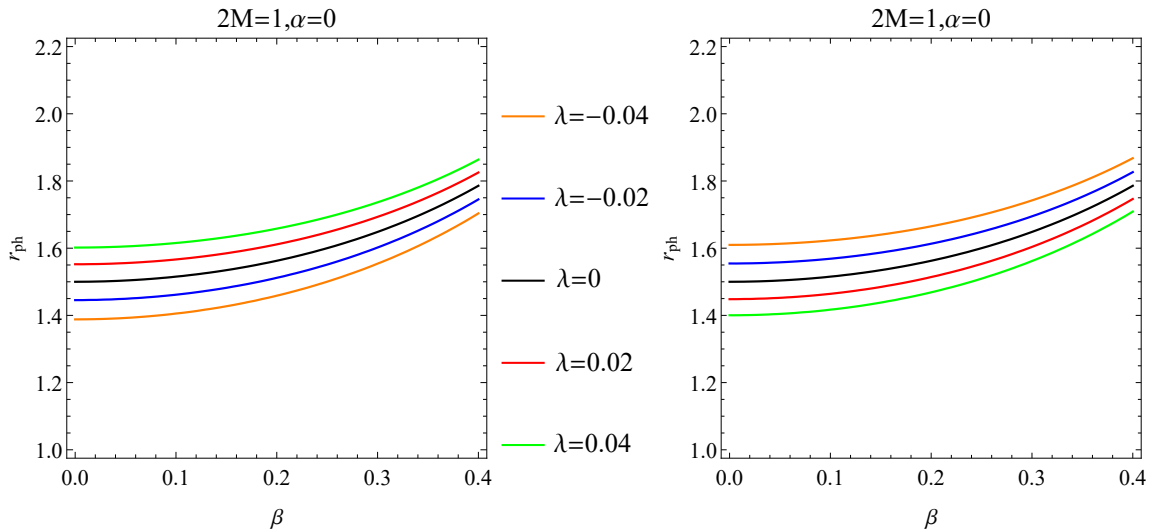


Figure 2. Variety of the photon sphere radius r_{ph} with the X-cold dark matter parameter β in a Brane-World black hole spacetime. The left and the right are for PPL and PPR, respectively.

increase of β , r_{ph} for a fixed value of the coupling parameter λ increases for two different coupled photons. In general, the photon sphere radius r_{ph} depends on the coupling parameter λ , β , and the polarization, which is quite different from that in the case without the coupling. In other words, the presence of the coupling leads to the diversity of the photon sphere radius r_{ph} .

B. Angular radius of the shadow

For the simplest case of a non-rotating black hole, the shadow is a circular disk in the sky. If the black hole is uncharged, it is to be modeled by the Schwarzschild metric. For a static observer in the spacetime of a Schwarzschild black hole, the angular radius of the shadow was calculated in a seminal paper by Synge [58]. Making use of this method, one can obtain the corrected angular radius of the shadow θ_{sh} in

the Brane-World black hole spacetime (2)

$$\sin^2\theta_{sh} = \frac{f(r_O) r_{ph}^2 W(r_O)}{f(r_{ph}) r_O^2 W(r_{ph})}. \quad (26)$$

Here, we assume that the observer is located at radius coordinate r_O with angular coordinate $\theta_O = \frac{\pi}{2}$.

As an example, we consider the supermassive black hole Sgr A* located at the Galactic center. The mass is estimated to be $M = 4.4 \times 10^6 M_\odot$ and its distance from the earth is around 8.5 kpc [59]. Substituting these data into the Eq. (26), the angular radius of the shadow yielded by the photons coupling with the Weyl tensor in the Brane-World spacetime are obtained and shown in Figs. 3 and 4.

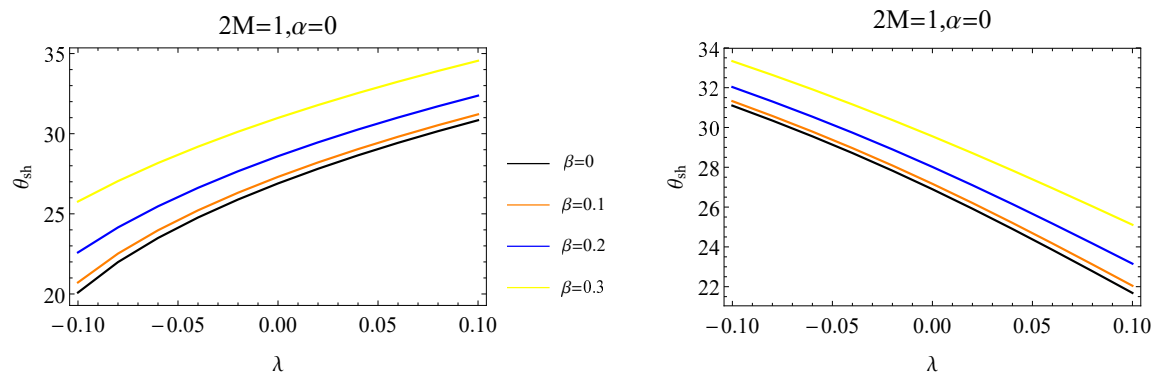


Figure 3. Variety of the angular radius of the shadow with the coupling constant λ in a Brane-World black hole spacetime. The left and the right are for PPL and PPR, respectively.

From Fig. 3, we find that for different β , the angular radius of the shadow θ_{sh} monotonically increases with the coupling parameter λ for PPL and decreases for PPR. In Fig. 4, with the increase of β , the angular radius of the shadow α_{sh} increases for two different coupled photons. Considering that due to the coupling photons with different polarization directions propagate along different paths in the

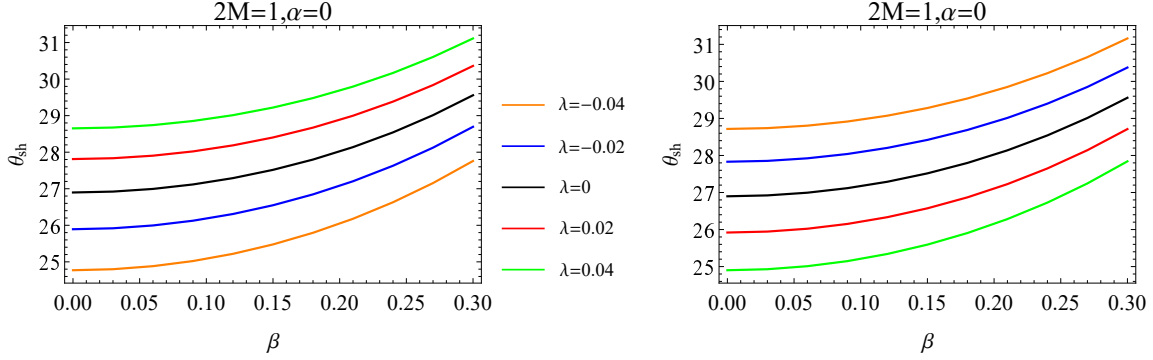


Figure 4. Variety of the angular radius of the shadow with the X-cold dark matter parameter β in a Brane-World black hole spacetime. The left and the right are for PPL and PPR, respectively.

spacetime, it is naturally expected that there exists a double shadow for a black hole as photons couple to the Weyl tensor. The overlap region of the double shadow is called an umbra. In Fig. 3, we see that, for different parameter β , the size of umbra is always determined by PPL when λ is negative and by PPR when λ is positive. Moreover, one can find that the umbra of the black hole increases with the X-cold dark matter parameter β and decreases with the coupling strength. And they coincide with the conclusions in Ref. [47]. In order to see more clearly the effect of β and the coupling parameter λ on the angular radius of penumbra of the black hole $\Delta\theta_{sh}$, we have made Fig. 5. It is shown that the size of penumbra increases with the coupling parameter λ and decreases with the X-cold dark matter parameter β . We can find that $\Delta\theta_{sh} = 0$ without the coupling, which means the double shadow of the black hole is reduced to a single shadow.

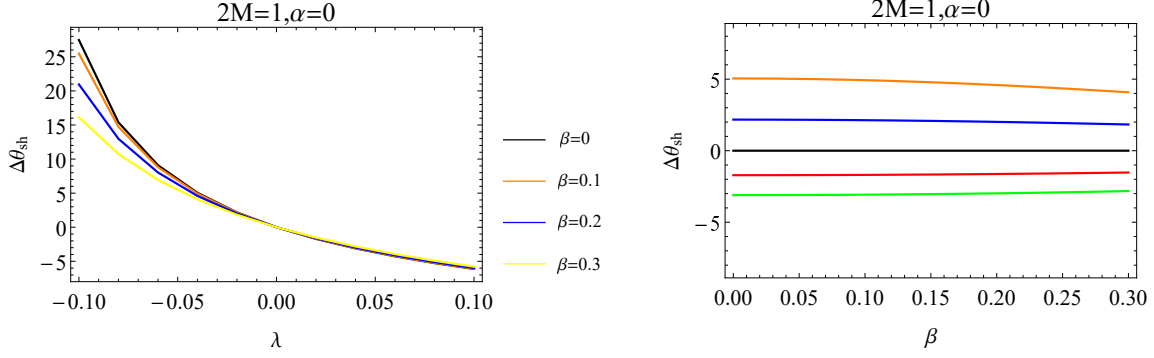


Figure 5. Evolution of the penumbra of the black hole with the coupling constant λ and the X-cold dark matter parameter β in the Brane-World black hole spacetime.

IV. DEFLECTION ANGLE OF LIGHT WITH FINITE-DISTANCE CORRECTIONS IN THE BRANE-WORLD BLACK HOLE

In this section, we proceed to study the deflection angle of light using the methodology given by Ishihara et al. [60, 61] under the assumption that the distance from the source (S) to the receiver (R) is finite.

Light rays satisfy the null condition as $ds^2 = 0$, which is rearranged as, via Eq. (20)

$$dt^2 = \tilde{\gamma}_{ij} dx^i dx^j = \frac{dr^2}{f^2(r)} + \frac{r^2}{W(r)f(r)}, \quad (27)$$

where i and j denote 1 and 2, $\tilde{\gamma}_{ij}$ is called the optical metric. The optical metric defines a 3-dimensional Riemannian space (denoted as M^{opt}), in which the light ray is expressed as a spatial curve. As usual, we define the impact parameter of the light ray as

$$b \equiv \frac{L}{E} = \frac{r^2}{W(r)f(r)} \frac{d\phi}{dt}. \quad (28)$$

By using Eqs. (27) and (28) by introducing a new variable as $u = r^{-1}$, one can obtain

the orbit equation as

$$\left(\frac{du}{d\phi}\right)^2 = \frac{1}{b^2W^2} - \frac{fu^2}{W} \equiv F(u). \quad (29)$$

Then, ϕ_{RS} is obtained as

$$\begin{aligned} \phi_{RS} = \int_S^R d\phi = & [\pi - \arcsin(bu_R) - \arcsin(bu_S)] + \frac{M}{b} \left(\frac{2 - b^2u_R^2}{\sqrt{1 - b^2u_R^2}} + \frac{2 - b^2u_S^2}{\sqrt{1 - b^2u_S^2}} \right) \\ & + \frac{8M\lambda}{b^3} \left(\frac{2 - b^2u_R^2}{\sqrt{1 - b^2u_R^2}} + \frac{2 - b^2u_S^2}{\sqrt{1 - b^2u_S^2}} \right) + \phi_1^*(\alpha, \beta, \lambda) \\ & + \mathcal{O} \left(bM^2u_R^3, bM^2u_S^3, \frac{M^2\lambda u_R^3}{b}, \frac{M^2\lambda u_S^3}{b}, \frac{M^2\lambda^2 u_R^3}{b^3}, \frac{M^2\lambda^2 u_S^3}{b^3}, b^3\alpha^2 u_R, b^3\alpha^2 u_S \right), \end{aligned} \quad (30)$$

for PPL and

$$\begin{aligned} \phi_{RS} = \int_S^R d\phi = & [\pi - \arcsin(bu_R) - \arcsin(bu_S)] + \frac{M}{b} \left(\frac{2 - b^2u_R^2}{\sqrt{1 - b^2u_R^2}} + \frac{2 - b^2u_S^2}{\sqrt{1 - b^2u_S^2}} \right) \\ & - \frac{8M\lambda}{b^3} \left(\frac{2 - b^2u_R^2}{\sqrt{1 - b^2u_R^2}} + \frac{2 - b^2u_S^2}{\sqrt{1 - b^2u_S^2}} \right) + \phi_2^*(\alpha, \beta, \lambda) \\ & + \mathcal{O} \left(bM^2u_R^3, bM^2u_S^3, \frac{M^2\lambda u_R^3}{b}, \frac{M^2\lambda u_S^3}{b}, \frac{M^2\lambda^2 u_R^3}{b^3}, \frac{M^2\lambda^2 u_S^3}{b^3}, b^3\alpha^2 u_R, b^3\alpha^2 u_S \right), \end{aligned} \quad (31)$$

for PPR, respectively. Here, the detailed forms of ϕ_1^* and ϕ_2^* are shown in the appendix.

Let Ψ denote the angle of the light ray measured from the radial direction. Accordingly, the Ψ_R and Ψ_S denote the angles that are measured at the receiver position (R) and the source position (S), respectively. Please see Fig. 6.

Using the unit tangent vector e_i along the light ray orbit in the space M^{opt} which satisfies the relation $\tilde{\gamma}_{ij}e^i e^j = 1$, we can obtain Ψ in terms of the following relation [60]

$$\sin \Psi = \frac{b\sqrt{Wf}}{r}. \quad (32)$$

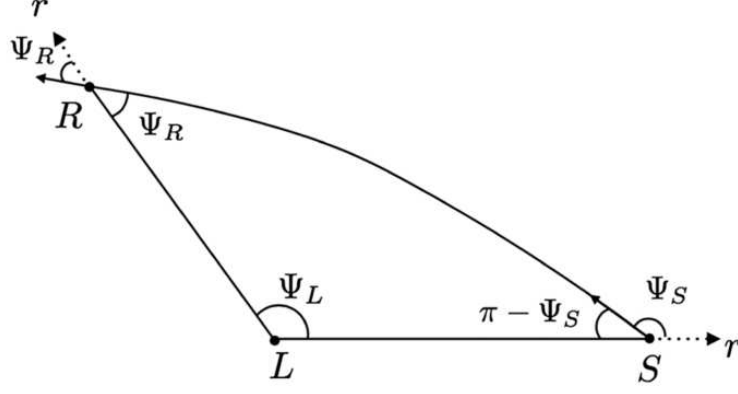


Figure 6. Triangle embedded in the curved space M^{opt} . Here, the point L denotes the lens center.

By Eq. (32), we find that $\Psi_R - \Psi_S$ for both PPL and PPR take this form under the low-order approximations:

$$\begin{aligned}
\Psi_R - \Psi_S = & \Phi_R^{Sch} - \Phi_S^{Sch} - \frac{b}{\sqrt{1-b^2u_R^2}} \left[\alpha\beta + \frac{\alpha^2}{2u_R} + \frac{\alpha^2 M}{2(1-b^2u_R^2)} \right] \\
& - \frac{b}{\sqrt{1-b^2u_S^2}} \left[\alpha\beta + \frac{\alpha^2}{2u_S} + \frac{\alpha^2 M}{2(1-b^2u_S^2)} \right] \\
& + \mathcal{O}(bM^2u_R^3, bM^2u_S^3, bM^2\alpha^2u_R, bM^2\alpha^2u_S, bM\alpha\beta u_R, bM\alpha\beta u_S, b\beta^2u_R, b\beta^2u_S),
\end{aligned} \tag{33}$$

where

$$\Phi_R^{Sch} - \Phi_S^{Sch} \equiv [\arcsin(bu_R) + \arcsin(bu_S) - \pi] - bM \left(\frac{u_R^2}{\sqrt{1-b^2u_R^2}} + \frac{u_S^2}{\sqrt{1-b^2u_S^2}} \right). \tag{34}$$

Let $\phi_{RS} \equiv \phi_R - \phi_S$ denote the coordinate separation angle between the receiver and source. Then the deflection angle $\hat{\alpha}$ is expressed as [60]

$$\hat{\alpha} \equiv \Psi_R - \Phi_S + \phi_{RS}, \tag{35}$$

where the closest approach $r_0 = u_0^{-1}$. That is to say, basically, one can find the

deflection angle $\hat{\alpha}$ by just computing Ψ_R , Ψ_S , and ϕ_{RS} and applying Eq. (35).

Inserting Eqs. (30), (31) and (33) into Eq. (35), the deflection angle can be obtained as

$$\begin{aligned}
\hat{\alpha} = & \frac{M}{b} \left(\frac{2 - b^2 u_R^2}{\sqrt{1 - b^2 u_R^2}} + \frac{2 - b^2 u_S^2}{\sqrt{1 - b^2 u_S^2}} \right) + \frac{8M\lambda}{b^3} \left(\frac{2 - b^2 u_R^2}{\sqrt{1 - b^2 u_R^2}} + \frac{2 - b^2 u_S^2}{\sqrt{1 - b^2 u_S^2}} \right) \\
& - M \left(\frac{b u_R^2}{\sqrt{1 - b^2 u_R^2}} + \frac{b u_S^2}{\sqrt{1 - b^2 u_S^2}} \right) - \frac{b\alpha^2}{2} \left(\frac{1}{u_R \sqrt{1 - b^2 u_R^2}} + \frac{1}{u_S \sqrt{1 - b^2 u_S^2}} \right) + \hat{\alpha}_1^* \\
& + \mathcal{O} \left(bM^2 u_R^3, bM^2 u_S^3, \frac{M^2 \lambda u_R^3}{b}, \frac{M^2 \lambda u_S^3}{b}, \dots, b\beta^2 u_R, b\beta^2 u_S \right),
\end{aligned} \tag{36}$$

for PPL. Similarly, for PPR, we have

$$\begin{aligned}
\hat{\alpha} = & \frac{M}{b} \left(\frac{2 - b^2 u_R^2}{\sqrt{1 - b^2 u_R^2}} + \frac{2 - b^2 u_S^2}{\sqrt{1 - b^2 u_S^2}} \right) - \frac{8M\lambda}{b^3} \left(\frac{2 - b^2 u_R^2}{\sqrt{1 - b^2 u_R^2}} + \frac{2 - b^2 u_S^2}{\sqrt{1 - b^2 u_S^2}} \right) \\
& - M \left(\frac{b u_R^2}{\sqrt{1 - b^2 u_R^2}} + \frac{b u_S^2}{\sqrt{1 - b^2 u_S^2}} \right) - \frac{b\alpha^2}{2} \left(\frac{1}{u_R \sqrt{1 - b^2 u_R^2}} + \frac{1}{u_S \sqrt{1 - b^2 u_S^2}} \right) + \hat{\alpha}_2^* \\
& + \mathcal{O} \left(bM^2 u_R^3, bM^2 u_S^3, bM^2 \alpha^2 u_R, bM^2 \alpha^2 u_S, bM\alpha\beta u_R, bM\alpha\beta u_S, b\beta^2 u_R, b\beta^2 u_S \right).
\end{aligned} \tag{37}$$

Here, the detailed forms of $\hat{\alpha}_1^*$ and $\hat{\alpha}_2^*$ are shown in the appendix.

Note that some terms in these two expressions may apparently diverge as $bu_R \rightarrow 0$ and $bu_S \rightarrow 0$. This is because the spacetime is not asymptotically flat and hence it does not allow the limit of $bu_R \rightarrow 0$ and $bu_S \rightarrow 0$. However, from a physical point of view, we know that an observed star or galaxy is located at a finite distance from us [60, 62]. In other words, we can consider only finitedistance corrections in this case, one can include only a certain finite distance which leads to the further

simplified relations

$$\hat{\alpha} \sim \frac{4M}{b} - \frac{b\alpha^2}{2} \left(\frac{1}{u_R} + \frac{1}{u_S} \right) + bM\alpha^2 + \frac{32M\lambda}{b^3} + \frac{48M^2\alpha\beta}{b} + \frac{8M\beta^2}{b} + \frac{768M^2\alpha\beta\lambda}{b^3} + \frac{256M\beta^2\lambda}{3b^3} + \frac{6144M^2\alpha\beta\lambda^2}{b^5} + \frac{1024M\beta^2\lambda^2}{3b^5}, \quad (38)$$

for PPL and

$$\hat{\alpha} \sim \frac{4M}{b} - \frac{b\alpha^2}{2} \left(\frac{1}{u_R} + \frac{1}{u_S} \right) + bM\alpha^2 - \frac{32M\lambda}{b^3} + \frac{48M^2\alpha\beta}{b} + \frac{8M\beta^2}{b} - \frac{768M^2\alpha\beta\lambda}{b^3} - \frac{256M\beta^2\lambda}{3b^3} + \frac{43008M^2\alpha\beta\lambda^2}{b^5} + \frac{7168M\beta^2\lambda^2}{15b^5}, \quad (39)$$

for PPR, respectively. Finally, we see that, when $\beta = 0$, $\lambda = 0$, and $\alpha^2 = \frac{\Lambda}{3}$, the deflection angle will reduce to the form in Kottler spacetime [60].

V. CONCLUSIONS AND DISCUSSIONS

In this paper, we have studied the equation of motion of the photon coupled to Weyl tensor by the geometric optics approximation and the corresponding shadow and weak gravitational lensing in a Brane-World black hole spacetime. Since the metric contains both dark energy parameter α and X-cold dark matter parameter β , we choose it as the background black hole spacetime. We find that the shadow and the gravitational lensing depend not only on the properties of background black hole spacetime, but also on the polarization of the coupled photon.

By calculating the shadow of the Brane-World black hole, we find that the photon sphere radius r_{ph} increases with the coupling parameter λ for PPL and decreases for PPR. And with the increases of β , r_{ph} increases for two different coupled photons. Moreover, we have investigated the double shadow of the black hole as photons

couple to the Weyl tensor, which does not appear in the non-coupling case where only a single shadow emerges. Combining with the supermassive central object in our Galaxy, we find the umbra of the black hole increases with the parameter β and decreases with the coupling strength. The dependence of the penumbra on the parameter β and the coupling strength is converse to that of the umbra.

We also study the gravitational deflection angle of light with finite-distance corrections in the weak deflection limit by means of a recent geometric method. Since the Brane-World black hole spacetime is nonasymptotically flat, the limit $bu_R \rightarrow 0$ and $bu_S \rightarrow 0$ is not allowed. However, it is not problematic because we can only observe a given star or a galaxy in finite distance from us.

Very recently, first images of the black hole M87 at the center of the Virgo A galaxy was obtained using the sub-millimeter “EHT” based on the VLBI [63]. We anticipate that future observations with highly improved techniques would be able to test our results by the observing the shadow and the deflection angle of the black hole.

CONFLICTS OF INTEREST

The authors declare that there are no conflicts of interest regarding the publication of this paper.

ACKNOWLEDGMENTS

We would like to thank the National Natural Science Foundation of China (Grant No.11571342) for supporting us on this work.

APPENDIX: EXPRESSIONS OF ϕ_1^* , ϕ_2^* , $\hat{\alpha}_1^*$ AND $\hat{\alpha}_2^*$

By using Eq. (29), ϕ_{RS} is expanded in a power series as Eq. (30) or Eq. (31), where

$$\begin{aligned}
\phi_1^* = & \frac{bM\alpha^2}{2} \left[\frac{2 - 3b^2u_R^2}{(1 - b^2u_R^2)^{\frac{3}{2}}} + \frac{2 - 3b^2u_S^2}{(1 - b^2u_S^2)^{\frac{3}{2}}} \right] + b\alpha\beta \left(\frac{1}{\sqrt{1 - b^2u_R^2}} + \frac{1}{\sqrt{1 - b^2u_S^2}} \right) \\
& + \frac{3M^2\alpha\beta}{b} \left[\frac{8 - 20b^2u_R^2 + 15b^4u_R^4}{(1 - b^2u_R^2)^{\frac{5}{2}}} + \frac{8 - 20b^2u_S^2 + 15b^4u_S^4}{(1 - b^2u_S^2)^{\frac{5}{2}}} \right] \\
& + \frac{M\beta^2}{2b} \left[\frac{8 - 12b^2u_R^2}{(1 - b^2u_R^2)^{\frac{3}{2}}} + \frac{8 - 12b^2u_S^2}{(1 - b^2u_S^2)^{\frac{3}{2}}} \right] \\
& + \frac{48M^2\alpha\beta\lambda}{b^3} \left[\frac{8 - 20b^2u_R^2 + 15b^4u_R^4}{(1 - b^2u_R^2)^{\frac{5}{2}}} + \frac{8 - 20b^2u_S^2 + 15b^4u_S^4}{(1 - b^2u_S^2)^{\frac{5}{2}}} \right] \\
& + \frac{64M\beta^2\lambda}{3b^3} \left[\frac{2 - 3b^2u_R^2}{(1 - b^2u_R^2)^{\frac{3}{2}}} + \frac{2 - 3b^2u_S^2}{(1 - b^2u_S^2)^{\frac{3}{2}}} \right] \\
& + \frac{384M^2\alpha\beta\lambda^2}{b^5} \left[\frac{8 - 20b^2u_R^2 + 15b^4u_R^4}{(1 - b^2u_R^2)^{\frac{5}{2}}} + \frac{8 - 20b^2u_S^2 + 15b^4u_S^4}{(1 - b^2u_S^2)^{\frac{5}{2}}} \right] \\
& + \frac{256M\beta^2\lambda^2}{3b^5} \left[\frac{2 - 3b^2u_R^2}{(1 - b^2u_R^2)^{\frac{3}{2}}} + \frac{2 - 3b^2u_S^2}{(1 - b^2u_S^2)^{\frac{3}{2}}} \right],
\end{aligned}$$

and

$$\begin{aligned}
\phi_2^* = & \frac{bM\alpha^2}{2} \left[\frac{2 - 3b^2u_R^2}{(1 - b^2u_R^2)^{\frac{3}{2}}} + \frac{2 - 3b^2u_S^2}{(1 - b^2u_S^2)^{\frac{3}{2}}} \right] + b\alpha\beta \left(\frac{1}{\sqrt{1 - b^2u_R^2}} + \frac{1}{\sqrt{1 - b^2u_S^2}} \right) \\
& + \frac{3M^2\alpha\beta}{b} \left[\frac{8 - 20b^2u_R^2 + 15b^4u_R^4}{(1 - b^2u_R^2)^{\frac{5}{2}}} + \frac{8 - 20b^2u_S^2 + 15b^4u_S^4}{(1 - b^2u_S^2)^{\frac{5}{2}}} \right] \\
& + \frac{M\beta^2}{2b} \left[\frac{8 - 12b^2u_R^2}{(1 - b^2u_R^2)^{\frac{3}{2}}} + \frac{8 - 12b^2u_S^2}{(1 - b^2u_S^2)^{\frac{3}{2}}} \right] \\
& - \frac{48M^2\alpha\beta\lambda}{b^3} \left[\frac{8 - 20b^2u_R^2 + 15b^4u_R^4}{(1 - b^2u_R^2)^{\frac{5}{2}}} + \frac{8 - 20b^2u_S^2 + 15b^4u_S^4}{(1 - b^2u_S^2)^{\frac{5}{2}}} \right]
\end{aligned}$$

$$\begin{aligned}
& - \frac{64M\beta^2\lambda}{3b^3} \left[\frac{2 - 3b^2u_R^2}{(1 - b^2u_R^2)^{\frac{3}{2}}} + \frac{2 - 3b^2u_S^2}{(1 - b^2u_S^2)^{\frac{3}{2}}} \right] \\
& + \frac{2688M^2\alpha\beta\lambda^2}{b^5} \left[\frac{8 - 20b^2u_R^2 + 15b^4u_R^4}{(1 - b^2u_R^2)^{\frac{5}{2}}} + \frac{8 - 20b^2u_S^2 + 15b^4u_S^4}{(1 - b^2u_S^2)^{\frac{5}{2}}} \right] \\
& + \frac{1792M\beta^2\lambda^2}{15b^5} \left[\frac{2 - 3b^2u_R^2}{(1 - b^2u_R^2)^{\frac{3}{2}}} + \frac{2 - 3b^2u_S^2}{(1 - b^2u_S^2)^{\frac{3}{2}}} \right].
\end{aligned}$$

Similarly, after some calculations, we have

$$\begin{aligned}
\hat{\alpha}_1^* &= \frac{bM\alpha^2}{2} \left[\frac{1 - 3b^2u_R^2}{(1 - b^2u_R^2)^{\frac{3}{2}}} + \frac{1 - 3b^2u_S^2}{(1 - b^2u_S^2)^{\frac{3}{2}}} \right] \\
& + \frac{3M^2\alpha\beta}{b} \left[\frac{8 - 20b^2u_R^2 + 15b^4u_R^4}{(1 - b^2u_R^2)^{\frac{5}{2}}} + \frac{8 - 20b^2u_S^2 + 15b^4u_S^4}{(1 - b^2u_S^2)^{\frac{5}{2}}} \right] \\
& + \frac{M\beta^2}{2b} \left[\frac{8 - 12b^2u_R^2}{(1 - b^2u_R^2)^{\frac{3}{2}}} + \frac{8 - 12b^2u_S^2}{(1 - b^2u_S^2)^{\frac{3}{2}}} \right] \\
& + \frac{48M^2\alpha\beta\lambda}{5b^3} \left[\frac{8 - 20b^2u_R^2 + 15b^4u_R^4}{(1 - b^2u_R^2)^{\frac{5}{2}}} + \frac{8 - 20b^2u_S^2 + 15b^4u_S^4}{(1 - b^2u_S^2)^{\frac{5}{2}}} \right] \\
& + \frac{64M\beta^2\lambda}{3b^3} \left[\frac{2 - 3b^2u_R^2}{(1 - b^2u_R^2)^{\frac{3}{2}}} + \frac{2 - 3b^2u_S^2}{(1 - b^2u_S^2)^{\frac{3}{2}}} \right] \\
& + \frac{384M^2\alpha\beta\lambda^2}{b^5} \left[\frac{8 - 20b^2u_R^2 + 15b^4u_R^4}{(1 - b^2u_R^2)^{\frac{5}{2}}} + \frac{8 - 20b^2u_S^2 + 15b^4u_S^4}{(1 - b^2u_S^2)^{\frac{5}{2}}} \right] \\
& + \frac{256M\beta^2\lambda^2}{b^5} \left[\frac{2 - 3b^2u_R^2}{(1 - b^2u_R^2)^{\frac{3}{2}}} + \frac{2 - 3b^2u_S^2}{(1 - b^2u_S^2)^{\frac{3}{2}}} \right],
\end{aligned}$$

and

$$\begin{aligned}
\hat{\alpha}_2^* &= \frac{bM\alpha^2}{2} \left[\frac{1 - 3b^2u_R^2}{(1 - b^2u_R^2)^{\frac{3}{2}}} + \frac{1 - 3b^2u_S^2}{(1 - b^2u_S^2)^{\frac{3}{2}}} \right] \\
& + \frac{3M^2\alpha\beta}{b} \left[\frac{8 - 20b^2u_R^2 + 15b^4u_R^4}{(1 - b^2u_R^2)^{\frac{5}{2}}} + \frac{8 - 20b^2u_S^2 + 15b^4u_S^4}{(1 - b^2u_S^2)^{\frac{5}{2}}} \right] \\
& + \frac{M\beta^2}{2b} \left[\frac{8 - 12b^2u_R^2}{(1 - b^2u_R^2)^{\frac{3}{2}}} + \frac{8 - 12b^2u_S^2}{(1 - b^2u_S^2)^{\frac{3}{2}}} \right]
\end{aligned}$$

$$\begin{aligned}
& - \frac{48M^2\alpha\beta\lambda}{5b^3} \left[\frac{8 - 20b^2u_R^2 + 15b^4u_R^4}{(1 - b^2u_R^2)^{\frac{5}{2}}} + \frac{8 - 20b^2u_S^2 + 15b^4u_S^4}{(1 - b^2u_S^2)^{\frac{5}{2}}} \right] \\
& - \frac{64M\beta^2\lambda}{3b^3} \left[\frac{2 - 3b^2u_R^2}{(1 - b^2u_R^2)^{\frac{3}{2}}} + \frac{2 - 3b^2u_S^2}{(1 - b^2u_S^2)^{\frac{3}{2}}} \right] \\
& + \frac{2688M^2\alpha\beta\lambda^2}{b^5} \left[\frac{8 - 20b^2u_R^2 + 15b^4u_R^4}{(1 - b^2u_R^2)^{\frac{5}{2}}} + \frac{8 - 20b^2u_S^2 + 15b^4u_S^4}{(1 - b^2u_S^2)^{\frac{5}{2}}} \right] \\
& + \frac{1792M\beta^2\lambda^2}{5b^5} \left[\frac{2 - 3b^2u_R^2}{(1 - b^2u_R^2)^{\frac{3}{2}}} + \frac{2 - 3b^2u_S^2}{(1 - b^2u_S^2)^{\frac{3}{2}}} \right].
\end{aligned}$$

REFERENCES

- [1] David Langlois. Brane cosmology. *Progress of Theoretical Physics Supplement*, 148:181–212, 2002.
- [2] Philippe Brax and Carsten van de Bruck. Cosmology and brane worlds: a review. *Classical and Quantum Gravity*, 20(9):R201, 2003.
- [3] Roy Maartens and Kazuya Koyama. Brane-world gravity. *Living Reviews in Relativity*, 13(1):5, 2010.
- [4] Valerii A Rubakov. Large and infinite extra dimensions. *Physics-Uspekhi*, 44(9):871, 2001.
- [5] C Csaki. Tasi lectures on extra dimensions and branes. arXiv. *hep-ph*, 404096, 2004.
- [6] Nima Arkani-Hamed, Savas Dimopoulos, and Gia Dvali. The hierarchy problem and new dimensions at a millimeter. *Physics Letters B*, 429(3-4):263–272, 1998.
- [7] Ignatios Antoniadis, Nima Arkani-Hamed, Savas Dimopoulos, and Gia Dvali. New dimensions at a millimeter to a fermi and superstrings at a tev. *Physics Letters B*, 436(3-4):257–263, 1998.

- [8] Lisa Randall and Raman Sundrum. Large mass hierarchy from a small extra dimension. *Physical Review Letters*, 83(17):3370, 1999.
- [9] Lisa Randall and Raman Sundrum. An alternative to compactification. *Physical Review Letters*, 83(23):4690, 1999.
- [10] Csaba Csaki, Michael Graesser, Christopher Kolda, and John Terning. Cosmology of one extra dimension with localized gravity. *Physics Letters B*, 462(1-2):34–40, 1999.
- [11] James M Cline, Christophe Grojean, and Geraldine Servant. Cosmological expansion in the presence of an extra dimension. *Physical Review Letters*, 83(21):4245, 1999.
- [12] M Heydari-Fard, H Razmi, and HR Sepangi. Brane-world black hole solutions via a confining potential. *Physical Review D*, 76(6):066002, 2007.
- [13] M Heydari-Fard and HR Sepangi. Anisotropic brane gravity with a confining potential. *Physics Letters B*, 649(1):1–11, 2007.
- [14] Malihe Heydari-Fard and HR Sepangi. Generalized chaplygin gas as geometrical dark energy. *Physical Review D*, 76(10):104009, 2007.
- [15] Ian T Drummond and SJ Hathrell. Qed vacuum polarization in a background gravitational field and its effect on the velocity of photons. *Physical Review D*, 22(2):343, 1980.
- [16] RD Daniels and Graham M Shore. faster than light photons and charged black holes. *Nuclear Physics B*, 425(3):634–650, 1994.
- [17] RD Daniels and Graham M Shore. faster than light photons and rotating black holes. *Physics Letters B*, 367(1-4):75–83, 1996.
- [18] Michael S Turner and Lawrence M Widrow. Inflation-produced, large-scale magnetic fields. *Physical Review D*, 37(10):2743, 1988.
- [19] Francisco D Mazzitelli and Federico M Spedalieri. Scalar electrodynamics and primordial magnetic fields. *Physical Review D*, 52(12):6694, 1995.

- [20] G Lambiase and AR Prasanna. Gauge invariant wave equations in curved space-times and primordial magnetic fields. *Physical Review D*, 70(6):063502, 2004.
- [21] Alfredo Raya, José Edgar Madriz Aguilar, and Mauricio Bellini. Gravitoelectromagnetic inflation from a 5D vacuum state: A new formalism. *Physics Letters B*, 638(4):314–319, 2006.
- [22] L Campanelli, P Cea, GL Fogli, and L Tedesco. Inflation-produced magnetic fields in $R^n F^2$ and IF^2 models. *Physical Review D*, 77(12):123002, 2008.
- [23] Kazuharu Bamba and Sergei D Odintsov. Inflation and late-time cosmic acceleration in non-minimal Maxwell- $F(R)$ gravity and the generation of large-scale magnetic fields. *Journal of Cosmology and Astroparticle Physics*, 2008(04):024, 2008.
- [24] K-T Kim, PP Kronberg, PE Dewdney, and TL Landecker. The halo and magnetic field of the Coma cluster of galaxies. *The Astrophysical Journal*, 355:29–37, 1990.
- [25] K-T Kim, Peter C Tribble, and PP Kronberg. Detection of excess rotation measure due to intracluster magnetic fields in clusters of galaxies. *The Astrophysical Journal*, 379:80–88, 1991.
- [26] Tracy E Clarke, Phil P Kronberg, and Hans Böhringer. A new radio-X-ray probe of galaxy cluster magnetic fields. *The Astrophysical Journal Letters*, 547(2):L111, 2001.
- [27] Adam Ritz and John Ward. Weyl corrections to holographic conductivity. *Physical Review D*, 79(6):066003, 2009.
- [28] Jian-Pin Wu, Yue Cao, Xiao-Mei Kuang, and Wei-Jia Li. The 3+ 1 holographic superconductor with Weyl corrections. *Physics Letters B*, 697(2):153–158, 2011.
- [29] Da-Zhu Ma, Yue Cao, and Jian-Pin Wu. The Stückelberg holographic superconductors with Weyl corrections. *Physics Letters B*, 704(5):604–611, 2011.
- [30] D Momeni, N Majd, and R Myrzakulov. p-wave holographic superconductors with Weyl corrections. *EPL (Europhysics Letters)*, 97(6):61001, 2012.

- [31] Dibakar Roychowdhury. Effect of external magnetic field on holographic superconductors in presence of nonlinear corrections. *Physical Review D*, 86(10):106009, 2012.
- [32] D Momeni, MR Setare, and Ratbay Myrzakulov. Condensation of the scalar field with Stuckelberg and Weyl Corrections in the background of a planar AdS-Schwarzschild black hole. *International Journal of Modern Physics A*, 27(22):1250128, 2012.
- [33] Davood Momeni and MR Setare. A note on holographic superconductors with Weyl corrections. *Modern Physics Letters A*, 26(38):2889–2898, 2011.
- [34] Zixu Zhao, Qiyuan Pan, and Jiliang Jing. Holographic insulator/superconductor phase transition with Weyl corrections. *Physics Letters B*, 719(4-5):440–447, 2013.
- [35] Songbai Chen and Jiliang Jing. Dynamical evolution of the electromagnetic perturbation with Weyl corrections. *Physical Review D*, 88(6):064058, 2013.
- [36] Songbai Chen and Jiliang Jing. Dynamical evolution of a vector field perturbation coupled to the einstein tensor. *Physical Review D*, 90(12):124059, 2014.
- [37] Hao Liao, Songbai Chen, and Jiliang Jing. Absorption cross section and hawking radiation of the electromagnetic field with Weyl corrections. *Physics Letters B*, 728:457–461, 2014.
- [38] SK Solanki, O Preuss, Mark P Haugan, A Gandorfer, HP Povel, P Steiner, K Stucki, PN Bernasconi, and D Soltau. Solar constraints on new couplings between electromagnetism and gravity. *Physical Review D*, 69(6):062001, 2004.
- [39] Oliver Preuss, Mark P Haugan, Sami K Solanki, and Stefan Jordan. An astronomical search for evidence of new physics: Limits on gravity-induced birefringence from the magnetic white dwarf RE J0317-853. *Physical Review D*, 70(6):067101, 2004.
- [40] Yakov Itin and Friedrich W Hehl. Maxwell’s field coupled nonminimally to quadratic torsion: Axion and birefringence. *Physical Review D*, 68(12):127701, 2003.
- [41] Tekin Dereli and Özcan Sert. Non-minimal $\ln(R)F^2$ Couplings of Electromagnetic Fields to Gravity: Static, Spherically Symmetric Solutions. *The European Physical*

Journal C, 71(3):1589, 2011.

- [42] Alexander B Balakin and José PS Lemos. Non-minimal coupling for the gravitational and electromagnetic fields: a general system of equations. *Classical and Quantum Gravity*, 22(9):1867, 2005.
- [43] Alexander B Balakin, Vladimir V Bochkarev, and José PS Lemos. Nonminimal coupling for the gravitational and electromagnetic fields: Black hole solutions and solitons. *Physical Review D*, 77(8):084013, 2008.
- [44] Friedrich W Hehl and Yuri N Obukhov. How does the electromagnetic field couple to gravity, in particular to metric, nonmetricity, torsion, and curvature? In *Gyros, Clocks, Interferometers...: Testing Relativistic Gravity in Space*, pages 479–504. Springer, 2001.
- [45] Songbai Chen and Jiliang Jing. Strong gravitational lensing for the photons coupled to weyl tensor in a schwarzschild black hole spacetime. *Journal of Cosmology and Astroparticle Physics*, 2015(10):002, 2015.
- [46] Songbai Chen, Shangyun Wang, Yang Huang, Jiliang Jing, and Shiliang Wang. Strong gravitational lensing for the photons coupled to a Weyl tensor in a kerr black hole spacetime. *Physical Review D*, 95(10):104017, 2017.
- [47] Yang Huang, Songbai Chen, and Jiliang Jing. Double shadow of a regular phantom black hole as photons couple to the Weyl tensor. *The European Physical Journal C*, 76(11):594, 2016.
- [48] G Abbas, Asif Mahmood, and M Zubair. Strong Gravitational Lensing for Photon Coupled to Weyl Tensor in Kiselev Black Hole. *arXiv preprint arXiv:1909.06433*, 2019.
- [49] Graham M Shore. Faster than Light Photons in Gravitational Fields II-Dispersion and Vacuum Polarisation. *Nuclear Physics B*, 633(1-2):271–294, 2002.

- [50] Rong-Gen Cai. Propagation of vacuum polarized photons in topological black hole spacetimes. *Nuclear Physics B*, 524(3):639–657, 1998.
- [51] Hing Tong Cho. “Faster Than Light” Photons in Dilaton Black Hole Spacetimes. *Physical Review D*, 56(10):6416, 1997.
- [52] VA De Lorenci, R de Klippert, M Novello, et al. Light propagation in non-linear electrodynamics [J]. *Phys. Lett. B*, 482:134–140, 2000.
- [53] Diego AR Dalvit, Francisco D Mazzitelli, and Carmen Molina-Paris. One-loop graviton corrections to Maxwell’s equations. *Physical Review D*, 63(8):084023, 2001.
- [54] N Ahmadi and M Nouri-Zonoz. Quantum gravitational optics: the induced phase. *Classical and Quantum Gravity*, 25(13):135008, 2008.
- [55] VA De Lorenci, Renato Klippert, M Novello, and JM Salim. Light propagation in non-linear electrodynamics. *Physics Letters B*, 482(1-3):134–140, 2000.
- [56] Sheperd S Doeleman, Jonathan Weintraub, Alan EE Rogers, Richard Plambeck, Robert Freund, Remo PJ Tilanus, Per Friberg, Lucy M Ziurys, James M Moran, Brian Corey, et al. Event-horizon-scale structure in the supermassive black hole candidate at the Galactic Centre. *Nature*, 455(7209):78, 2008.
- [57] NS Kardashev, VV Khartov, VV Abramov, V Yu Avdeev, AV Alakoz, Yu A Aleksandrov, S Ananthakrishnan, VV Andreyanov, AS Andrianov, NM Antonov, et al. radioastron-a telescope with a size of 300 000 km: Main parameters and first observational results. *Astronomy Reports*, 57(3):153–194, 2013.
- [58] JL Synge. The escape of photons from gravitationally intense stars. *Monthly Notices of the Royal Astronomical Society*, 131(3):463–466, 1966.
- [59] Reinhard Genzel, Frank Eisenhauer, and Stefan Gillessen. The galactic center massive black hole and nuclear star cluster. *Reviews of Modern Physics*, 82(4):3121, 2010.
- [60] Asahi Ishihara, Yusuke Suzuki, Toshiaki Ono, Takao Kitamura, and Hideki Asada. Gravitational bending angle of light for finite distance and the gauss-bonnet theorem.

Physical Review D, 94(8):084015, 2016.

- [61] Toshiaki Ono, Asahi Ishihara, and Hideki Asada. Gravitomagnetic bending angle of light with finite-distance corrections in stationary axisymmetric spacetimes. *Physical Review D*, 96(10):104037, 2017.
- [62] Sumarna Haroon, Mubasher Jamil, Kimet Jusufi, Kai Lin, and Robert B Mann. Shadow and deflection angle of rotating black holes in perfect fluid dark matter with a cosmological constant. *Physical Review D*, 99(4):044015, 2019.
- [63] Kazunori Akiyama, Antxon Alberdi, Walter Alef, Keiichi Asada, Rebecca Azulay, Anne-Kathrin Baczko, David Ball, Mislav Baloković, John Barrett, Dan Bintley, et al. First M87 Event Horizon Telescope Results. IV. Imaging the Central Supermassive Black Hole. *The Astrophysical Journal Letters*, 875(1):L4, 2019.